Neural Network Based Structural Damage Detection In Steel Plates Using Time And Frequency Domain Features

M. P. Paulraj, Sazali Yaacob, Mohd Shukry Abdul Majid and R. Prenesh Krishnan

Abstract- This paper presents detection of damages in steel plates using time domain and frequency domain features are presented. A simple experimental model is developed based on two dissimilar boundary conditions to hold the steel plate. Experimental methods are developed to excite the steel plate at one corner of the cell and measure the responsive vibration signal at the adjacent coordinates of the cell. The vibration signal is then blocked into number of frames of definitive size. Feature extraction algorithms are developed to extract the following features namely: frame energy based features, DCT peak moment, change in DCT peak moment, DCT peak value derivative and DCT peak area. The feature vectors are then associated with the condition of the steel plate. A simple radial basis function network is modeled and trained using the extracted features to classify the condition of the steel plate using 60%, 70% and 80% training samples and tested with 100% testing samples. The performance of the network is validated using normal and Falhman testing method and the results are tabulated.

Keywords: Vibration signal, Experimental modal analysis, damage detection, neural networks, radial basis function, frame energy, discrete cosine transformation.

I. INTRODUCTION

Health monitoring of vibrating structure in machines is an important task in industries. Damages can put human safety at risk, cause long term machine downtimes, interruption in the production and subsequently increase the production cost. Early damage detection and possible location of the faults from the vibration measurements is one of the primary tasks of condition monitoring. Condition monitoring enables early detection of faults. In recent years there has been an increasing interest in the development of online condition monitoring systems due to the success in several applications. Structural Health Monitoring (SHM) is an inverse problem which mainly concentrates on damage existence, damage localization and damage extent measurement. The purpose of SHM is to ensure high reliability and less maintenance cost throughout the lifetime of the structure. A damage condition of a steel plate can be detected by the vibration signal propagating through it, when it is subjected to an impulse force. There are many technologies that have been developed to detect the faults in a gear box, bridge structures, aircraft and bearings with the aid of vibration signals. The existence of a crack in a steel plate reduces the stiffness of the plate and this reduction in stiffness ultimately reduces the natural frequencies. Further, this also changes the mode shape of vibration. An analysis of the propagation of the vibration signal makes it possible to detect the fault non-destructively.

An extensive literature review of the state of art vibration analysis and damage detection has been published by S.W. Doebling [1]. A detailed survey of the state of art in the damage detection field using modal analysis has been presented by Richardson [2]. A detailed review of the different vibration and acoustic methods such as the time and frequency domains, acoustic emission techniques are presented by Tandon and Nakra [3]. Using fracture mechanics method, Dimarogonas [4] and Anifactis [5] computed the equivalent stiffness and developed a model for crack detection in beams. An experimental technique to estimate the location and depth of a crack in a beam has been developed by Adams and Cawley [6]. An unidentified damage in steel plates can degrade the lifespan of the product. To ensure long life, the condition of the steel plate needs to be monitored. Nondestructive vibration testing methods for damage identification gains more importance in the recent past.

In this work, two types of experimental arrangements are proposed based on the boundary conditions. The vibration signals are captured from the stainless steel plate in pre and post damage conditions. The vibration signal is processed to extract features namely frame energy based statistical features and discrete cosine transformation features. These extracted features are then associated with the healthy or faulty condition of the steel plate. Radial basis function network models are developed and trained using the extracted features. The performance of the network is validated and the results are tabulated. This paper, is organized in the following subsections; the experimental design, feature extraction and the artificial neural networks for classification are explained in the corresponding subsections.

II. EXPERIMENTAL ARRANGEMENT

2.1. Data acquisition system

Measurements of the vibration signals are acquired using a LMS SCADAS Mobile SCM01 Data Acquisition

M.P.Paulraj, School of Mechatronic Engineering, Universiti Malaysia Perlis, Ulu Pauh Campus, Arau, 02600, Perlis, Malaysia.

Sazali Yaacob, School of Mechatronic Engineering, Universiti Malaysia Perlis, Ulu Pauh Campus, Arau, 02600, Perlis, Malaysia.

Mohd Shukry Abdul Majid, School of Mechatronic Engineering, Universiti Malaysia Perlis, Ulu Pauh Campus, Arau, 02600, Perlis, Malaysia.

R. Prenesh Krishnan, School of Mechatronic Engineering, Universiti Malaysia Perlis, Ulu Pauh Campus, Arau, 02600, Perlis, Malaysia.

ISBN 978-1-4507-5679-2@ 2011 Published by the Coimbatore Institute of Information Technology

System. This system has 4 input channels and Ethernet connectivity. The features supported are: a maximum sampling frequency range of up to 102.4 kHz per channel, 105 dB signal to noise ratio and a high speed Ethernet connection. The DAQ system is monitored through the LMS Test Lab software which supports a wide range of applications.

2.2. Vibration and pressure transducers

Accelerometers are Vibration transducers which possess high natural frequencies compared to the vibration to be measured and indicate acceleration. The piezoelectric accelerometers are widely preferred over the digital accelerometers in many applications due to its high accuracy and sensitivity. The general purpose Piezoelectric accelerometer with an input sensitivity of 10 / 31.6 / 100mV/g (g = 9.82 m/s2) and a resonant frequency of 28 kHz is used in this experimental work. Force transducers are used to produce impulse forces and commonly used for impact tests. The general purpose force transducers or so called impact hammer (Dytran 5800B2 - 50LbF range, 100 mV/LbF) is used in this research work.

2.3. Experimental setup

A clean 2B Stainless steel plate of length 60 cms, breadth 24 cms and thickness 0.12 cms are subjected for this testing. The steel plate is divided into 6 rows and 15 columns forming a grid structure of cell size 4x4 cm^2 as shown in the Figure 1.1. The cells of 6 rows and 6 columns are numbered sequentially as represented in Figure 1.2. Two simple experimental test setups are fabricated to test and evaluate the condition of the steel structure using Nondestructive Experimental Modal Analysis (NDEMA).

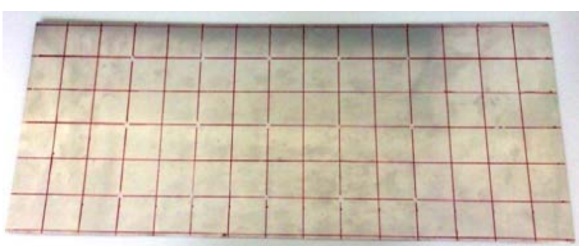

Figure.1 1 Stainless Steel Plate divided into cells

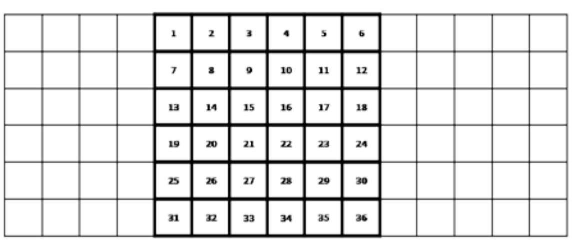

Figure.1.2 Grid formation of the steel structure

2.4. Simply supported steel plate

An aluminium test rig of length 90 cms, breadth 60 cms and height 3 cms is fabricated. The rectangular stainless steel plate of mass 1.2 kilogram is freely placed over the test setup. The plate is simply supported by two thin threads tied across the test bench 30 cms apart from each other as shown in Figure 1.3. The test setup is placed on a rubber mattress to avoid external vibrations.

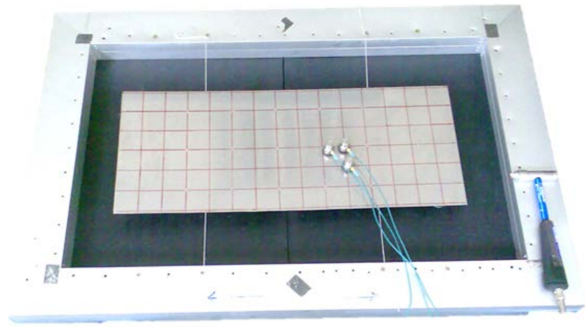

Figure.1.3. Experimental Test Setup of Steel Plate Simply Supported

2.5. Fixed free steel plate

An Iron swing frame setup of height 5 feet and width 3 feet is constructed. The Stainless Steel plate is clamped and hinged between the two holders while the other end of the steel plate is set free as shown in the Figure 1.4. The distance between the two holders is 40 cms.

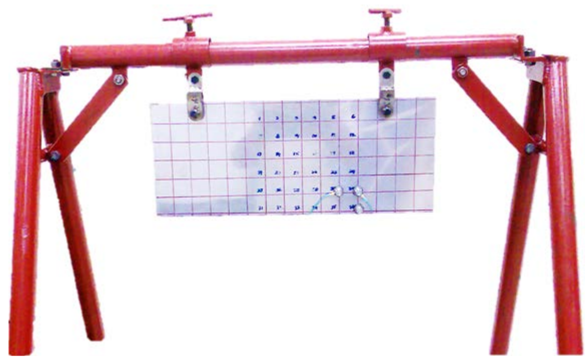

Figure.1.4. Experimental Test Setup of Steel Plate Hinged one side

2.7. Data capturing protocol design

Based on the physical properties of the steel plate such as natural frequency, mode shape, the sampling frequency is set to 4 kHz [16]. The impact hammer is connected to the first ICP channel of the Data Acquisition System. Three general purpose mono axis accelerometers are connected to the second, third and fourth ICP channels respectively. An impulse force is generated by striking the impact hammer on a nodal point on the steel plate. The vibration generated due to the external impulse force is propagated throughout the plate. The level of vibration at the nearest three nodal points is measured using the accelerometers.

The placement of the accelerometers and the location of strike are now changed at the same cell as represent are depicted in the Figures 1.5, 1.6, 1.7 and 1.8 respectively. The impulse force and the level of vibration at the nearest locations are recorded for 20 seconds at a sampling rate of 4 kHz [7]. This procedure is executed in all the 36 cells and 10 such trials are applied during the healthy condition of the stainless steel plate.

Small drilled holes of diameter between 512 μm to 1852 μm and depth of 100 μm are manually made using drill bits on the surface of the steel plate. The damages are made in all the 36 cells which constitute 144 possible locations. The vibration signal from the steel plate during the fault condition is captured using the same procedure. The experiment is repeated and the vibration signal is obtained from 10 steel plates of similar dimensions. Thus 1440 samples are captured and recorded for normal conditions. Similarly 1440 samples for fault conditions including minimum, medium and maximum damages are collected after drilling small holes on the steel plates. The experimental data collected using simply supported and fixed free method comprises of 2880 samples each respectively.

These captured signals are in default file format '.xdf' of the Data acquisition system, which are then exported as Microsoft '.wav' file format for further analysis through MATLAB.

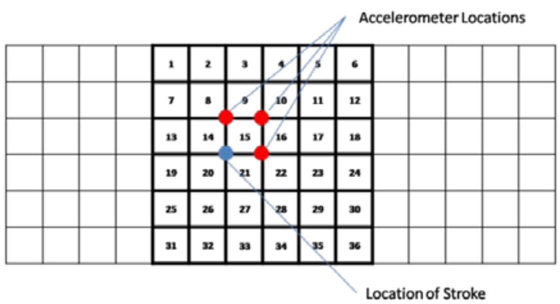

Figure.1.5.Location of Strike – Protocol 1

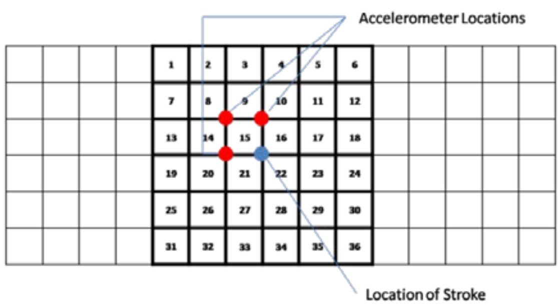

Figure.1.6.Location of Strike – Protocol 2

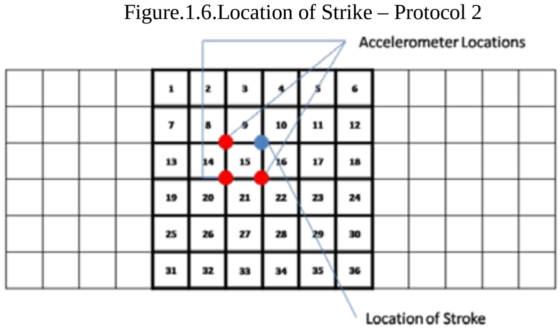

Figure.1.7.Location of Strike – Protocol 3

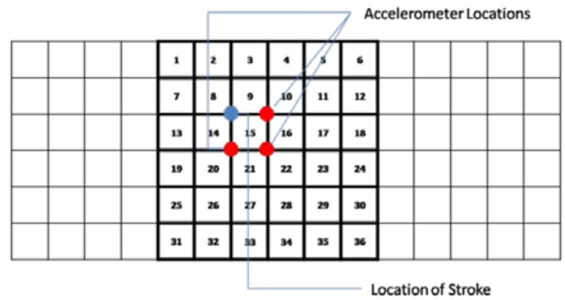

Figure.1.8.Location of Strike – Protocol 4

III. FEATURE EXTRACTION

The vibration response signal recorded from the accelerometers contains the time verses amplitude information for a time stamp of 20 seconds. In this research, the features from the vibration signals are extracted in both time and frequency domains. Algorithms are developed to extract frame energy based features and discrete cosine transformation based features. The feature extraction process is explained in suitable subsections of this paper.

3.1 Frame blocking

To effectively study the features, the vibration signal is decomposed into definite frames of size 1024. The vibration signal is recorded for 20 seconds while the time of strike of the impact hammer is inconsistent. Hence to maintain uniformity of the signal length, the signal corresponding to 15 seconds is extracted using the signal trimming procedure.

3.1.1. Signal trimming procedure

The transient vibration signal is recorded for 20 seconds during the impact testing process. The time 't_p' corresponding to the first peak magnitude 'v_p' is identified. The vibration signal recorded from (t_p – 0.5) seconds to (t_p + 14.5) seconds are extracted. The period of the resulting extracted signal is 15 seconds and is used for further analysis. The energy of the signal is the sum of the squared magnitudes. A typical representation of the vibration signal blocked into frames is represented in Figure 1.9.

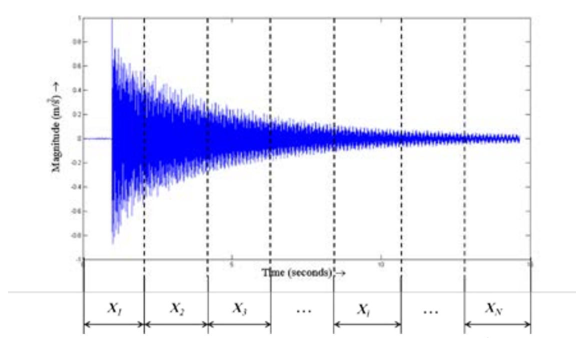

Figure 1.9: A typical vibration signal blocked into frames

3.2. Frame energy based features

To study the change in the energy decay, the following frame energy based statistical features namely: kurtosis, root mean square, total delta energy and number of slope changes are extracted from the signal.

3.2.1. Kurtosis (K)

The Kurtosis K is defined as the fourth moment of the distribution and measure of the size of the tails of distribution. The kurtosis feature is extracted using the Equation (1.1).

$$K = \frac{1}{N}\sum_{i=1}^{N}\left(\frac{e_i - e_\mu}{e_\sigma}\right)^4 \qquad (1.1)$$

where $e_i = i^{th}$ frame energy,

e_μ = overall mean frame energy,

e_σ = standard deviation of frame energy and

N = total number of frames.

3.2.2. Root Mean Square (E_{rms})

The Root Mean Square is the time domain analysis feature which is a measure of the power content in the vibration signature. The Root Mean Square (E_{rms}) is calculated using Equation (1.2).

$$E_{rms} = \sqrt{\frac{1}{N}\sum_{i=1}^{N} e_i} \qquad (1.2)$$

where $e_i = i^{th}$ frame energy and

N = total number of frames.

3.2.3 Total Delta Energy (ΔE)

The vibration response is a function of energy decay with respect to time. The sum of the change in energy between two successive frames in the signal is referred to as the total delta energy (ΔE) and is computed using Equation (1.3).

$$\Delta E = \sum_{i=2}^{N-1}\left(e_{i-1} - e_i\right) \qquad (1.3)$$

where $e_i = i^{th}$ frame energy,

i = frame number and

N = total number of frames.

3.2.4 Number of slope changes (ΔS)

The vibration response of the frames decays exponentially with respect to time. The slope of the energy decay depends on the plate condition and hence the frame energy values between two successive frames are compared and the changes in slope values are computed. If the product of two consecutive frame energies is less than zero then it is considered as a slope change. The total number of slope changes computed from the frame energy values constitutes a feature. The equations for computing the number of slope changes are expressed in Equations (1.4) and (1.5)

$$\Delta S = \sum_{i=1}^{N-2} f\left(\Delta e_{i+1} * \Delta e_i\right) \qquad (1.4)$$

$$f\left(\Delta e_{i+1} * \Delta e_i\right) = \begin{cases} 1 & if\ \left(\Delta e_{i+1} * \Delta e_i\right) < 0 \\ 0 & if\ \left(\Delta e_{i+1} * \Delta e_i\right) \geq 0 \end{cases} \qquad (1.5)$$

Δe_i = change in frame energy of the i^{th} frame and

$f\left(\Delta e_{i+1} * \Delta e_i\right)$ is the slope change.

Using the frame energy based feature extraction method, 12 features are extracted from 1440 normal and 1440 fault samples. The feature vectors are then associated with the condition (normal or fault) of the steel plate.

3.3 Discrete cosine transformation based features

To study the change in frequency content of the normal and damaged conditions, the vibration signal is transformed into frequency domain. Discrete cosine transformation is applied over the frame energies calculated from the vibration signal. The extracted DCT coefficients ***D*** are represented in Equations (1.6) and (1.7) respectively. A typical representation of the discrete cosine transformation coefficients are shown in Figure 1.10.

$$\boldsymbol{D} = \left(abs\left(dct\left(\boldsymbol{E}\right)\right)\right) \qquad (1.6)$$

$$\boldsymbol{D} = \left[D_1, D_2, D_3, \ldots, D_i, \ldots, D_N\right] \qquad (1.7)$$

where $D_i = i^{th}$ absolute DCT component and

N = number of absolute DCT coefficients.

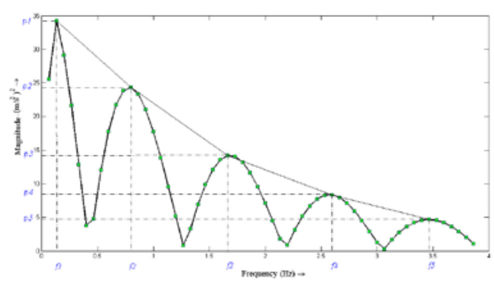

Figure 1.10: A typical representation of DCT peak magnitudes and frequency indices

The peak values ***P*** and its corresponding frequency indices ***f*** are extracted from the absolute values of the DCT coefficients and are represented in Equations (1.8) and (1.9) respectively.

$$\boldsymbol{P} = \left[p_1, p_2, p_3, \ldots, p_i, \ldots, p_q\right] \qquad (1.8)$$

$$\boldsymbol{f} = \left[f_1, f_2, f_3, \ldots, f_i, \ldots, f_q\right] \qquad (1.9)$$

where $p_1, p_2, p_3, \ldots, p_i, \ldots, p_q$ are the peak magnitudes,

$f_1, f_2, f_3, \ldots, f_i, \ldots, f_q$ are corresponding frequency indices of the peak magnitudes.

q = total number of peak magnitudes = total number of frequency indices.

To effectively study the change in the frequency information, the following Discrete cosine transformation features are extracted.

3.3.1. DCT peak moment

The DCT peak moment ***M*** is the product of the DCT peak magnitudes ***P*** and its corresponding frequency index ***f*** and is shown in Equation (1.10).

$$\boldsymbol{M} = \lfloor p_1 f_1, p_2 f_2, p_3 f_3, \ldots, p_i f_i, \ldots, p_q f_q \rfloor \quad (1.10)$$

where $\boldsymbol{M}$ denotes the DCT peak moment and

q = total number of peak magnitudes = total number of frequency indices.

Using the DCT peak moment feature extraction method, nine features are extracted from 1440 normal and 1440 fault samples. The feature vectors are then associated with the condition (normal or fault) of the steel plate.

3.3.2. Change in DCT peak moment

The change in DCT peak moments between successive DCT peak moments are calculated using Equations (1.11) and (1.12).

$$\boldsymbol{\Delta M} = \lfloor \Delta M_1, \Delta M_2, \Delta M_3, \ldots, \Delta M_i, \ldots, \Delta M_{q-1} \rfloor \quad (1.11)$$

where

$$\Delta M_i = \left(p_{i+1} f_{i+1} - p_i f_i\right) \quad (1.12)$$

q = total number of moments.

Using the change in DCT peak moment feature extraction method, nine features are extracted from 1440 normal and 1440 fault samples. The feature vectors are then associated with the condition (normal or fault) of the steel plate.

3.3.3 DCT peak value derivative

The DCT peak values decays along with their frequency indices. The rate of change of DCT peak values varies significantly in the steel plates with damages. The rate of change of the DCT peak magnitude and the frequency indices are extracted using Equation (1.14).

$$\boldsymbol{\Delta r} = \lfloor \Delta r_1, \Delta r_2, \Delta r_3, \ldots, \Delta r_i, \ldots, \Delta r_{q-1} \rfloor \quad (1.13)$$

where $\Delta r_i = i^{th}$ peak value derivative coefficient.

$$\Delta r_i = \frac{\Delta p_i}{\Delta f_i} \quad (1.14)$$

where $\Delta p_i = \left(p_i - p_{i+1}\right)$ and (1.15)

$$\Delta f_i = \left(f_{i+1} - f_i\right). \quad (1.16)$$

Using the DCT peak derivative feature extraction method, nine features are extracted from 1440 normal and 1440 fault samples. The feature vectors are then associated with the condition (normal or fault) of the steel plate.

3.3.4 DCT peak area

The successive DCT peak coefficients are connected by straight lines. The area swept by the consecutive DCT peak moments are computed and used as features to classify the normal and faulty steel locations. The area of trapezoids $\boldsymbol{A}$ is computed using the base formula (area of the trapezoid) shown in Equation (1.18)

$$\boldsymbol{A} = \lfloor A_1, A_2, A_3, \ldots, A_i, \ldots, A_{q-1} \rfloor \quad (1.17)$$

where

$$A_i = \left(\frac{1}{2} b_i h_i\right), \quad (1.18)$$

$b_i = \left(f_{i+1} - f_i\right)$ and (1.19)

$$h_i = \left(p_i + p_{i+1}\right) \quad (1.20)$$

Using the DCT peak area feature extraction method, nine features are extracted from 1440 normal and 1440 fault samples. The feature vectors are then associated with the condition (normal or fault) of the steel plate.

IV. DATA PREPROCESSING

The data preprocessing involves labeling of inputs and outputs, identification and removal of outliers, feature selection, data dimensionality reduction and data normalization. The feature matrix is rescaled to a definite range using a normalization criterion to improve speed and reduce complexity during classification. The input data samples are associated with their corresponding output vector and fed to the classifier model for classification. To represent the normal condition of the steel plate, the input features are mapped to ‘0.1’ and to represent the fault condition in the steel plate, the input features are mapped to ‘0.9’. The outlier present in the dataset when unidentified distorts the mean and variance which further leads to poor classification results. Outliers are removed from the dataset using five point summary method. In this research work softmax normalization is used.

TABLE 1.1: DIMENSIONALITY REDUCTION FOR SIMPLY SUPPORTED

		Original Features	Principal Component Features
Feature Extraction Methods	Frame energy	12	8
	DCT peak moments	12	10
	Change in DCT peak moment	9	9
	DCT peak value derivative	9	7
	DCT peak area	9	6

TABLE 1.2: DIMENSIONALITY REDUCTION FOR FIXED FREE

		Original Features	Principal Component Features
Feature Extraction Methods	Frame energy	12	9
	DCT peak moments	12	8
	Change in DCT peak moment	9	6
	DCT peak value derivative	9	8
	DCT peak area	9	9

Principal component analysis is employed to reduce dimensionality of the data by identifying principal component features [8]. The principal component features are extracted for the simply supported and the fixed free experimental methods and are tabulated in Tables 4.5 and 4.6 respectively. The data is then randomized and the training and testing database are formulated.

V. CLASSIFICATION USING RADIAL BASIS FUNCTION NETWORK

5.1Artificial neural network

An artificial neural network is an information processing system that has been developed as a generalization of the mathematical model for human cognition [9]. Artificial Neural Networks (ANN) provides alternative form of computing that attempts to mimic the functionality of the brain [10]. A Radial Basis Function (RBF) network model is developed and trained using the features extracted from the vibration signal.

5.2Radial basis function network

Radial basis function networks are developed to classify the condition of the steel plate. The network models are trained using the features extracted from the steel plate. The radial basis function network consists of three layers namely: input layer, hidden layer and output layer. The input layer is fed with the feature vectors extracted from the vibration signal. The hidden layer also referred to as the kernel layer determines the number of kernels. The input patterns from the input layer are nonlinearly transformed and fed as input to the hidden layer. In the hidden layer, the kernels (radial basis functions) are established and the weight vectors are governed. The weight vectors are adjusted based on the spread factor and the basis function. The ‘newrb’ function present in the MATLAB Neural network toolbox is used to model and train the RBF models. The newrb function iteratively adds one neuron at a time until the sum squared error falls behind the error goal or until the maximum number of hidden neurons are reached.

5.2.1. Neural network testing and validation

From the final feature matrix 60%, 70% and 80% samples of the total dataset are randomly chosen to train the network models. The performance of the network models namely the classification accuracy, sensitivity, specificity and number of kernels is calculated by validating the network with 100% samples of the dataset. During the validation of the trained neural network, the actual output is compared across the desired output with a testing tolerance. In this work, the ‘threshold and margin criterion’ devised by Scott E. Falhman [11] is considered. In this method the output classes: class1 and class2 are associated to 0.1 and 0.9 respectively. The threshold value is set in such a way that, the output values of the simulated network lying between 0 to 0.3 is considered as 0.1 (class1) and output values lying between 0.7 to 0.9 is considered to be 0.9 (class2). The target output values above 0.3 and below 0.7 are considered ‘marginal’ and are not considered as correct during training. The neural network training results are tested using this method and are compared with the normal testing method.

VI. RESULTS AND DISCUSSION

The consolidated training parameters of the RBF network models developed for the simply supported and fixed free experimental methods are tabulated in Tables 1.3 and 1.4 respectivey.

TABLE 1.3: COMPARISON OF RBF NETWORK ARCHITECTURE (SIMPLY SUPPORTED)

Feature Extraction methods		Frame energy	DCT peak moments	Change in DCT peak moment	DCT peak value derivative	DCT peak area
Training Parameters	Input Neurons	8	10	9	7	6
	Spread	0.5	0.5	0.5	0.5	0.5
	Output Neurons	1	1	1	1	1
	Goal	0.01	0.01	0.01	0.01	0.01
	Testing Tolerance	0.1	0.1	0.1	0.1	0.1
	Testing Samples	2764	2795	2746	2800	2782

TABLE 1.4: COMPARISON OF RBF NETWORK ARCHITECTURE (FIXED FREE)

Feature Extraction methods		Frame energy	DCT peak moments	Change in DCT peak moment	DCT peak value derivative	DCT peak area
Training Parameters	Input Neurons	9	8	6	9	9
	Spread	0.5	0.5	0.5	0.5	0.5
	Output Neurons	1	1	1	1	1
	Goal	0.01	0.01	0.01	0.01	0.01
	Testing Tolerance	0.1	0.1	0.1	0.1	0.1
	Testing Samples	2814	2804	2798	2810	2776

The RBF network models developed for the simply supported and fixed free experimental methods using the features extracted from the vibration signals are trained iteratively for 25 times per each trail. Five such trials are carried out and the minimum, mean and maximum of classification accuracy are tabulated in Tables 1.5 and 1.6 respectively.

TABLE 1.5: COMPARISON OF MEAN CLASSIFICATION ACCURACY FOR RBF NETWORK MODELS (SIMPLY SUPPORTED)

Feature Extraction Methods	Mean classification accuracy					
	Normal testing			Falhman testing		
	60%	70%	80%	60%	70%	80%
Frame energy	86.08	89.64	91.44	92.74	93.97	95.38
DCT peak moment	88.81	91.17	93.06	92.98	94.04	95.24
Change in DCT peak moment	87.70	89.60	92.45	91.47	92.78	95.24
DCT peak value derivative	87.95	88.35	92.59	92.15	93.47	94.65
DCT peak area	89.81	90.85	92.20	94.15	95.63	97.71

TABLE 1.6: COMPARISON OF MEAN CLASSIFICATION ACCURACY FOR RBF NETWORK MODELS (FIXED FREE)

Feature Extraction Methods	Mean classification accuracy					
	Normal testing			Falhman testing		
	60%	70%	80%	60%	70%	80%
Frame energy	91.07	92.75	93.40	92.30	93.26	95.33
DCT peak moment	89.31	91.13	93.15	92.98	93.47	94.91
Change in DCT peak moment	88.30	88.60	90.08	92.98	94.13	94.77
DCT peak value derivative	90.50	91.61	93.77	95.42	96.06	97.07
DCT peak area	90.88	91.99	94.08	96.06	96.17	98.89

The minimum, mean and maximum sensitivity for the RBF models developed for the simply supported and fixed free experimental methods for the feature extraction methods are tabulated in Tables 1.7 and 1.8 respectively.

TABLE 1.7: COMPARISON OF MEAN SENSITIVITY FOR RBF NETWORK MODELS (SIMPLY SUPPORTED)

Feature Extraction Methods	RBF mean network sensitivity					
	Normal Testing			Falhman Testing		
	60%	70%	80%	60%	70%	80%
Frame energy	86.20	90.16	91.46	93.32	93.88	96.18
DCT peak moment	88.81	91.17	93.06	92.40	93.89	95.16
Change in DCT peak moment	88.00	90.14	92.92	91.81	93.62	95.19
DCT peak value derivative	87.26	88.00	92.70	91.19	93.96	94.20
DCT peak area	90.51	90.56	92.34	94.18	96.25	98.23

TABLE 1.8: COMPARISON OF MEAN SENSITIVITY FOR RBF NETWORK MODELS (FIXED FREE)

Feature Extraction Methods	RBF mean network sensitivity					
	Normal Testing			Falhman Testing		
	60%	70%	80%	60%	70%	80%
Frame energy	91.25	93.34	93.80	92.41	93.45	96.13
DCT peak moment	89.96	91.15	93.30	93.81	93.83	95.67
Change in DCT peak moment	88.60	89.24	90.20	92.98	94.13	94.77
DCT peak value derivative	90.00	91.23	93.15	95.16	95.87	97.35
DCT peak area	91.08	92.84	94.30	97.41	96.78	99.82

The minimum, mean and maximum specificity for the RBF models developed for the simply supported and fixed free experimental methods for the feature extraction methods are tabulated in Tables 1.9 and 1.10 respectively.

TABLE 1.9: COMPARISON OF MEAN SPECIFICITY FOR RBF NETWORK MODELS (SIMPLY SUPPORTED)

Feature Extraction Methods	RBF mean network sensitivity					
	Normal Testing			Falhman Testing		
	60%	70%	80%	60%	70%	80%
Frame energy	85.98	89.12	91.43	92.16	93.24	94.58
DCT peak moment	88.68	91.01	93.15	92.15	93.11	94.15
Change in DCT peak moment	87.58	89.08	91.98	91.13	91.94	95.29
DCT peak value derivative	88.64	88.70	92.48	93.11	93.98	95.10
DCT peak area	89.11	91.14	92.06	94.12	95.01	97.20

TABLE 1.10: COMPARISON OF MEAN SPECIFICITY FOR RBF NETWORK MODELS (FIXED FREE)

Feature Extraction Methods	RBF mean network sensitivity					
	Normal Testing			Falhman Testing		
	60%	70%	80%	60%	70%	80%
Frame energy	90.89	92.16	93.00	92.19	93.07	94.53
DCT peak moment	88.66	91.01	93.00	92.15	93.11	94.15
Change in DCT peak moment	87.00	88.96	89.98	92.17	93.82	94.16
DCT peak value derivative	91.00	91.99	94.39	95.68	96.25	96.79
DCT peak area	90.68	91.14	93.86	94.71	95.53	97.96

The minimum and maximum number of mean kernels for RBF models developed for the simply supported and fixed free experimental methods for the feature extraction methods are tabulated in Tables 1.11 and 1.12 respectively.

TABLE 1.11: COMPARISON OF MEAN KERNELS FOR RBF MODELS (SIMPLY SUPPORTED)

Feature Extraction Methods	Training Samples		
	60%	70%	80%
Frame energy	560	583	602
DCT peak moment	524	550	600
Change in DCT peak moment	540	554	616
DCT peak value derivative	606	636	679
DCT peak area	603	642	691

TABLE 1.12: COMPARISON OF MEAN KERNELS FOR RBF MODELS (FIXED FREE)

Feature Extraction Methods	Training Samples		
	60%	70%	80%
Frame energy	512	527	552
DCT peak moment	525	536	579
Change in DCT peak moment	552	554	573
DCT peak value derivative	472	523	560
DCT peak area	576	607	632

VII. CONCLUSION AND FUTURE WORK

This paper presented two simple experimental methods based on nondestructive experimental model analysis to extract vibration signals from the steel plate. Feature extraction algorithms based on time and frequency domain methods were developed to extract features from the recorded vibration signals. The features were then associated with the condition of the steel plate to form the final feature matrix. Radial basis network models were developed and trained to classify the condition of the steel plate. The results show that the network models developed using the fixed free experimental models perform better classification compared to the simply supported experimental method. The Falhman testing method provides better classification results compared to the normal testing method. Furthermore, the RBF network models developed and trained using the DCT peak are method provide better classification results in both the experimental methods.

REFERENCES

[1] S.W.Doebling, C.R. Farrar and M.B. Prime (1998), A summary review of vibration based damage identification methods, The Shock and Vibration Digest 30(2), pp 91-105.

[2] Richardson MH (1980), Detection of damage in structures from changes in their dynamic (modal) properties – a survey, NUREG/CR-1931, U.S. Nuclear Regulatory Commission, Washington, District of Calumbia.

[3] Tandon N, Nakra B C, Vibration and acoustic monitoring technique for detection of defects in rolling element bearings a review, Shock and Vibration Digest 1992, 24(3), pp 3-11.

[4] A.Dimarogonas, Vibration Engineering, West Publishes, St.Paul, Minesota, 1976.

[5] N.Anifantis, P.Rizos, A.Dimarogonas, Identification of cracks by vibration analysis, American society of Mechanical Engineers, Design Division Publications DE 7 (1985), pp 189-197.

[6] A.D.Adams, P.Cawley, The location of defects in structures from measurements of natural frequencies, Journal of Strain analysis 14 (1979) pp 49-57.

[7] Sophocles J. Orfanidis, Introduction to Signal Processing, pg 7-10, Prentice Hall 1996.

[8] KL Priddy and PE Keller, Artificial Neural Networks – An Introduction, SPIE Press, 2005.

[9] Simon Haykin, Neural Networks- A Comprehensive Foundation, Prentice Hall, 2002.

[10] S.N Sivanandam and Paulraj M, An Introduction to Artificial Neural Networks, Vikhas Publication , India, 2003.

[11] Falhman, S. E. (1998). An empirical study of learning speed in backpropagation Networks, CMU-CS-88-162.